Author Manuscript

Author Manuscript

Author Manuscript

Author Manuscript

HHS Public Access

Author manuscript

Free Radic Biol Med. Author manuscript; available in PMC 2017 December 01.

Published in final edited form as:

Free Radic Biol Med. 2016 December ; 101: 32–43. doi:10.1016/j.freeradbiomed.2016.09.019.

MnTE-2-PyP modulates thiol oxidation in a hydrogen peroxide-mediated manner in a human prostate cancer cell

Qiang Tong[a,b], **Yuxiang Zhu**[a], **Joseph W. Galaske**[a], **Elizabeth A. Kosmacek**[a], **Arpita Chatterjee**[a], **Bryan C. Dickinson**[c], and **Rebecca E. Oberley-Deegan**[a,*]

[a]Department of Biochemistry and Molecular Biology, University of Nebraska Medical Center, Omaha, NE, 68198, USA

[b]Department of Gastrointestinal Surgery, Union Hospital, Tongji Medical College, Huazhong University of Science and Technology, Wuhan, 430022, China

[c]Department of Chemistry, The University of Chicago, Chicago, Illinois 60637, USA

Abstract

To improve the treatment of advanced prostate cancer, the development of effective and innovative antitumor agents is needed. Our previous work demonstrated that the ROS (reactive oxygen species) scavenger, MnTE-2-PyP, inhibited human prostate cancer growth and also inhibited prostate cancer migration and invasion. We showed that MnTE-2-PyP treatment altered the affinity of the histone acetyltransferase enzyme, p300, to bind to DNA. We speculate that this may be one mechanism by which MnTE-2-PyP inhibits prostate cancer progression. Specifically, MnTE-2-PyP decreased p300/HIF-1/CREB complex (p300/hypoxia-inducible factor-1/cAMP response element-binding protein) binding to a specific hypoxia-response element (HRE) motif within the plasminogen activator inhibitor-1 (PAI-1) gene promoter region, and consequently, repressed PAI-1 expression. However, it remains unclear how MnTE-2-PyP reduces p300 complex binding affinity to the promoter region of specific genes. In this study, we found that overexpression of Cu/ZnSOD (superoxide dismutase 1, SOD1) significantly suppressed PAI-1 gene expression and p300 complex binding to the promoter region of PAI-1 gene, just as was observed in cells treated with MnTE-2-PyP. Furthermore, catalase (CAT) overexpression rescued the inhibition of PAI-1 expression and p300 binding by MnTE-2-PyP. Taken together, the above findings suggest that hydrogen peroxide (H_2O_2) is likely the mediator through which MnTE-2-PyP inhibits the PAI-1 expression and p300 complex binding in PC3 cells. To confirm this, we measured the production of H_2O_2 following overexpression of SOD1 or catalase with MnTE-2-PyP treatment in the presence or absence of radiation. We found that MnTE-2-PyP increased the intracellular steady-state levels of H_2O_2 and increased nuclear H_2O_2 levels. As expected, catalase overexpression significantly decreased the levels of intracellular H_2O_2 induced by MnTE-2-PyP. We then

*Address Correspondence: Department of Biochemistry and Molecular Biology, #7014 DRC1, 985870 Nebraska Medical Center, Omaha, NE 68106, Phone: (402)-559-9364, becky.deegan@unmc.edu.

Publisher's Disclaimer: This is a PDF file of an unedited manuscript that has been accepted for publication. As a service to our customers we are providing this early version of the manuscript. The manuscript will undergo copyediting, typesetting, and review of the resulting proof before it is published in its final citable form. Please note that during the production process errors may be discovered which could affect the content, and all legal disclaimers that apply to the journal pertain.

Conflicts of interest statement: Dr. Oberley-Deegan is a consultant with BioMimetix Pharmaceutical, Inc. and hold equities in BioMimetix Pharmaceutical, Inc. There are no conflicts of interest for the other authors.

Author Manuscript Author Manuscript Author Manuscript Author Manuscript

determined if this increased H_2O_2 production could result in oxidized protein thiol groups. In the presence of MnTE-2-PyP, there was a significant increase in oxidized thiols in PC3 cell lysates and this was reversed with catalase overexpression. Specifically, we showed that p300 was oxidized after MnTE-2-PyP treatment, indicating that MnTE-2-PyP is creating a more oxidizing environment and this is altering the oxidation state of p300 thiol residues. Our data provide an in depth mechanism by which MnTE-2-PyP regulates gene transcription through induced H_2O_2 mediated oxidation of particular proteins, supporting an important role for MnTE-2-PyP as an effective and innovative antitumor agent to enhance treatment outcomes in prostate cancer radiotherapy.

Keywords

MnTE-2-PyP; p300; Cu/ZnSOD; prostate cancer; hydrogen peroxide (H_2O_2)

INTRODUCTION

Prostate cancer is the second most commonly diagnosed cancer and the second leading cause of cancer death for men in the United States [1]. Of the individuals diagnosed with prostate cancer, roughly half will undergo radiotherapy for treatment [2]. Although radiation effectively kills tumor cells, it also damages nearby healthy tissues. Radiotherapy for prostate cancer can cause severe long-term complications that include bowel and rectal wall damage, urinary urgency and frequency, erectile dysfunction, urethral stricture, and incontinence [3, 4]. Therefore, to improve radiation therapy-induced quality of life impairments, it is imperative to develop more effective therapies and innovative agents to protect normal tissues from radiation damage, while at the same time inhibiting tumor progression.

Over the past decade, efforts to develop several new radioprotectors have been made. These drugs profoundly reduce the damage in normal tissues caused by radiation and have shown promising results at the preclinical stage [5]. However, most of them have limited clinical application either because of acute and chronic toxicities, or because they protect tumors as well as normal tissues from radiation. For example, a free radical scavenger, Amifostine, has been tested in Phase III clinical trials for head and neck cancer, non-small cell lung cancer and pelvic malignancies [6], and the American Society of Clinical Oncology recommended it as a radioprotectant in cancer radiotherapy [7]. Unfortunately, several reports of tumor protection from radiation damage along with numerous side effects have greatly limited its broader clinical use [8, 9].

MnTE-2-PyP (chemical name: Manganese (III) Meso-Tetrakis-(N-Ethylpyridinium-2-yl) scavenges reactive oxygen species (ROS), including superoxide, lipid peroxides and peroxynitrite. Along with its antioxidant properties, MnTE-2-PyP can act as a potent anti-inflammatory agent that inhibits NF-κB activity [10]. Furthermore, MnTE-2-PyP has been found to protect normal tissue from radiation damage. In particular, MnTE-2-PyP protects from erectile dysfunction and testicular atrophy after irradiation exposure to the urogenital region [11]. In order for MnTE-2-PyP to be considered a good radioprotector for cancer

Author Manuscript Author Manuscript Author Manuscript Author Manuscript

radiotherapy, it is fully necessary to explore whether MnTE-2-PyP can protect prostate tumor cells from radiation induced killing. Rabbani *et al.* showed that in combination with radiation, MnTE-2-PyP inhibits both tumor growth and tumor angiogenesis in mouse mammary cancer cells [12]. MnTE-2-PyP also sensitizes human prostate cells to radiation [13]. Thus, these reports above demonstrate that MnTE-2-PyP could be used clinically as a radioprotector and radiosensitizer for the treatment of cancer radiotherapy.

We have previously explored the mechanisms by which MnTE-2-PyP inhibits human prostate cancer progression alone and in combination with radiation. In that study, we determined that MnTE-2-PyP decreased p300/HIF-1/CREB complex (p300/hypoxia-inducible factor-1/cAMP response element-binding protein) binding to a specific hypoxia-response element (HRE) motif within the plasminogen activator inhibitor-1 (PAI-1) gene promoter region, suppressed H3K9 acetylation, and as a result repressed PAI-1 expression [13]. However, we still do not understand the mechanism by which MnTE-2-PyP reduces the p300 complex binding affinity for the promoter region of PAI-1.

Therefore, the current study was undertaken to determine the mechanism(s) by which MnTE-2-PyP reduces the p300 transcriptional complex binding affinity for DNA. We found that the overexpression of Cu/ZnSOD (superoxide dismutase 1, SOD1) could mimic MnTE-2-PyP activity, indicating that MnTE-2-PyP dismutes superoxide to hydrogen peroxide (H_2O_2). Accordingly, the overexpression of catalase in MnTE-2-PyP treated cells, resulted in enhanced p300 transcriptional complex binding to DNA. These data indicated that H_2O_2 may be the key molecule through which MnTE-2-PyP inhibits the p300 complex binding to DNA in PC3 cells. Indeed, MnTE-2-PyP treatment resulted in a 2-fold increase in intracellular steady state H_2O_2 levels as compared to untreated cells. Specifically, MnTE-2-PyP enhanced H_2O_2 levels in the nuclear compartment. We then showed that MnTE-2-PyP treatment results in the oxidation of many proteins, including the thiol groups on the p300 protein. We speculate that these oxidized thiols on p300 result in less affinity of the p300 transcriptional complex for the DNA. This is the first study to demonstrate that MnTE-2-PyP produces high levels of H_2O_2 intracellularly, specifically in the nucleus. It is also the first study to show that MnTE-2-PyP can indirectly oxidize p300. These studies are crucial in determining how MnTE-2-PyP regulates the expression of cancerous genes and can be better used for the treatment of prostate cancer.

MATERIALS AND METHODS

Cell culture and reagents

Human prostate cancer cell line, PC3, was purchased from American Type Culture Collection (ATCC). PC3 cells were cultured in RPMI-1640 media containing L-glutamine, 10% fetal bovine serum and 1% penicillin/streptomycin, in a 37°C incubator containing 95% air and 5% CO_2. Cells were passed before reaching confluency by detachment with trypsin 0.25% (1 ×) solution (HyClone) and were passed less than 30 times. NBT (nitroblue tetrazolium), DTT (dithiothreitol), BIAM [N- (Biotinoyl) - N'- (Iodoacetyl) Ethylenediamine], and H_2O_2 were from Fisher Scientific (Pittsburgh, PA, USA). Ferric chloride, potassium ferricyanide, catalase from bovine liver, diamide, TEMED (N, N, N', N'-tetramethyl-ethylenediamine), 3-aminotriazole, riboflavin and β-mercaptoethanol were

Author Manuscript Author Manuscript Author Manuscript Author Manuscript

purchased from Sigma-Aldrich (St. Louis, MO, USA). MnTE-2-PyP was provided by Dr. James Crapo, National Jewish Health, Denver, CO.

Catalase and SOD1 transfection of PC3 cells

The replication-defective recombinant type 5 adenovirus containing human catalase or SOD1 DNA was used in this experiment. The cDNAs are under the control of the human CMV (cytomegalovirus) promoter. Ad5CMVCAT and Ad5CMVSOD1 were produced by the University of Iowa Viral Vector Core (http://www.medicine.uiowa.edu/vectorcore). Human catalase cDNA or SOD1 cDNA was Inserted into the E1 region of an adenovirus construct which has a deletion of the entire E1 and partial E3 regions, which renders the recombinant adenovirus replication-deficient. An adenoviral vector without reporter gene (VQAd/Empty) was used as a negative control (produced by ViraQuest Inc., North Liberty, IA). Human PC3 cells (1.0×10^6) were plated in 10 mL of complete media in a 100 mm^2 tissue culture dish and allowed to attach for 24 hours. Cells were then washed three times in serum- and antibiotic-free media. The adenovirus constructs (Ad5CMVCAT, Ad5CMVSOD1 and VQAd/Empty) were applied to PC3 cells with 0, 50, 100,150 or 200 MOI (multiplicity of infection) in 4 mL of low serum media (2% fetal bovine serum). Cells were incubated with the adenovirus constructs for 4 hours followed by recovery in full media with 10% fetal bovine serum for an additional 72 hours.

Western blot

PC3 cells were homogenized in a cell lysis buffer containing 120 mM NaCl, 50 mM Tris-HCl, 5 mM EDTA, 1% NP-40 and complete protease inhibitor cocktail tablets (Roche, 1 tablet/50 ml) and incubated for 30 minutes on ice. Homogenates were then centrifuged at 4°C for 10 minutes at 10,000 g, and supernatants collected. Nuclear extracts were isolated from PC3 cells with the CelLytic NuCLEAR Extraction Kit (Sigma-Aldrich). Protein concentrations were measured using a Bradford assay (Amresco, Solon, OH, USA). Samples with equal amounts of protein were separated by Bolt 4-12% Bis-Tris Plus gels (Thermo Fisher Scientific) and transferred to polyvinylidene difluoride membranes (Life Technologies, Grand Island, NY, USA). After incubation with 5% nonfat milk in TBST (10 mM Tris, pH 8.0, 150 mM NaCl, 0.5% Tween 20) overnight at 4°C, the membrane was washed once with TBST and incubated with antibodies against catalase (R&D Systems, Minneapolis, MN, USA) (1:5000), SOD1 (gift from Dr. Rick Domann, University of Iowa, IA) (1:5000), or Histone H1 (Abcam, Cambridge, MA, USA) (1:1000) at room temperature for 1 h. Membranes were then washed with TBST three times for 10 min each and incubated with a 1:10000 dilution of HRP-conjugated goat anti-rabbit antibody (Life Technologies) for 1 hour at room temperature. Blots were washed with TBST five times for 10 min each, developed with an ECL detection system (Thermo Scientific), and exposed to films.

Immunofluorescence

PC3 cells were transfected with 200 MOI adenovirus constructs (Ad5CMVCAT, Ad5CMVSOD1 and VQAd/Empty) and 3×10^4 cells per chamber were seeded into 8-chamber culture slides (Falcon, USA). The next day, cells were rinsed with ice-cold PBS and fixed with 4% paraformaldehyde for 10 minutes at room temperature followed by permeabilization with 0.5% Triton-X100 in PBS for 5 minutes. The cells were subjected to

Author Manuscript Author Manuscript Author Manuscript Author Manuscript

immunofluorescence staining with catalase antibody (Abcam) (1:50) or SOD1 antibody (gift from Dr. Rick Domann, University of Iowa, IA) (1:100) for 1 hour at room temperature. The cells were then washed with cold PBS three times for 3 minutes each, and incubated with 100μl 20μM Alexa Fluor-488 goat anti-rabbit IgG conjugate antibody (Life Technologies) at 37°C for 1 hour protected from light. After 4'-6' diamidino-2-phenylindole (DAPI) (Sigma-Aldrich) staining, the cells were examined by a fluorescence microscope (Leica, DM4000 B LED). Images were selected from six random microscopic fields.

SOD1 and catalase activity staining assay

SOD1 and catalase activity assays were performed as described previously [14, 15]. Briefly, 2.0×10^6 PC3 cells were homogenized in a cell lysis buffer containing 120 mM NaCl, 50 mM Tris-HCl, 5 mM EDTA, 1% NP-40 and complete protease inhibitor cocktail tablets (1 tablet/50 ml) and incubated for 30 minutes on ice. Homogenates were then centrifuged at 4°C for 10 minutes at 10,000 g, and supernatants collected. SOD1 and catalase activity were measured by separating 25 μg of proteins on a 10% Mini-PROTEAN TGX precast gel (Bio-Rad), constant 100 V for 2 hour at room temperature under native conditions. For SOD, following electrophoresis, the gel was placed in the dark and incubated with 2.43 mM nitroblue tetrazolium (NBT), 28 μM riboflavin, and 28 mM TEMED for 20 minutes. After washing excessively with distilled water, the gel was then exposed to fluorescent light for several minutes. Areas of SOD1 activity appeared as achromatic bands in blue background. For measuring catalase activity, the electrophoresed gel was extensively rinsed with distilled water three times, for 10 minutes each and then soaked in 0.003% H_2O_2 for 10 minutes. A staining solution consisting of 2% ferric chloride and 2% potassium ferricyanide was then added. Areas of catalase activity appears as clear (negative staining) bands on a blue-green background.

Real-time Quantitative PCR

Approximately 6.0×10^5 adenovirus transfected PC3 cells were pretreated with 30 μM MnTE-2-PyP overnight, and then exposed to 20 Gy of radiation. 24 hours later, RNA was then isolated from PC3 cells with the ZR RNA MicroPrep RNA isolation kit (Zymo Research, Irvine, CA, USA) according to the manufacturer's protocol. For quantitative analysis of PAI-1 gene mRNA expression, comparative real-time PCR was performed with the use of Power SYBR Green RNA-to-CT 1 step kit (Applied Biosystems, Foster City, CA, USA). Quantitative PCR was performed under the following conditions: 48°C for 30 min, 95°C for 10 min, then 40 cycles with 95°C for 15 sec and 60°C for 1 min. Following the final cycle, the melt curves of the PCR products were determined to verify the integrity of the PCR products. The sequences for the amplification of human PAI-1 were: 5'-ACCGCAACGTGGTTTTCTCA-3' (forward) and 5'-TTGAATCCCATAGCTGCTTGAAT-3' (reverse). 18S rRNA was used as an external endogenous standard. The forward, 5'-CGGCTACATCCAAGGAA-3', and reverse, 5'-GCTGGAATTACCGCGGCT-3'.

p300 Chromatin Immuno-precipitation (ChIP) assay

ChIP assays were performed as described previously [16]. Briefly, after pretreatment with MnTE-2-PyP (30 μM) overnight, PC3 cells with or without adenovirus transfection were

Author Manuscript Author Manuscript Author Manuscript Author Manuscript

exposed to 20 Gy of radiation. One hour later, 1.0×10^7 cells were fixed with 1% of formaldehyde. Genomic DNA was sheared to lengths ranging from 200 to 1000 bp with a Sonic Dismembrator (Fisher Scientific): Ampl 80%, 3 seconds on, 10 seconds off, for 10 cycles. One percent of the cell extract was taken as "input", and the rest of the extract was incubated with either anti-p300 (Santa Cruz, Santa Cruz, CA, USA), or control IgG (Santa Cruz) overnight at 4°C, followed by precipitation with protein A agarose beads (EMD Millipore, Billerica, MA, USA). The immunoprecipitates were sequentially washed with a low salt buffer, a high salt buffer, a LiCl buffer, and with TE buffer. The DNA-protein complex was eluted and proteins were then digested with proteinase K. The DNA was detected by real-time quantitative PCR analysis and the data obtained by real-time PCR for each specific antibody were normalized to IgG control and plotted as percent input. ChIP primers for HRE (hypoxia response element) in the human PAI-1 gene promoter (−194 to −187 bp) was: (forward, 5'-CAGAAAGGTCAAGGGAGGTTC-3' and reverse, 5'-CTGCTCTGTGTGTGTACGTGTG-3').

Intracellular hydrogen peroxide levels assayed by aminotriazole-mediated inactivation of catalase

The intracellular steady-state levels of H_2O_2 can be estimated by using a sensitive assay based on 3-aminotriazole inhibition of catalase [17-19]. Briefly, PC3 cells were transfected with the adenovirus constructs (Ad5CMVCAT, Ad5CMVSOD1 and VQAd/Empty) and treated with or without MnTE-2-PyP, then placed in full media containing 10% FBS with 0 or 20 mM 3-aminotriazole at 37°C. At specified time points (0, 2.5, 5, 10, 15, 20 min), cells were rinsed two times with 5.0 mL ice-cold 50 mM phosphate buffered saline (PBS), pH 7.4 and then scrape-harvested into 1.0 mL of the same buffer, centrifuged at 300 g, then 200 μl of 50 mM phosphate buffer pH 7 was added to the pellets and frozen at −20°C. H_2O_2 concentration was calculated by kinetic analysis of the rate of decrease of catalase activity [17]. For catalase activity assays, the cell pellets were thawed rapidly in warm, not hot, flowing tap water and then sonicated 5 times until the pellet "disappeared" with a Sonic Dismembrator (Fisher Scientific): Ampl 50%, 1 second on, 3 seconds off. Protein concentrations were quantified by a Bradford assay (Amresco). Spectrophotometric catalase activities were run as described [20] using 80 μg homogenate cellular protein in phosphate buffer, pH 7.0 (total volume 200 μl). The assay was initiated by the addition of 100 μl of a 30 mM H_2O_2 stock solution in phosphate buffer, pH 7.0, and the loss of absorbance at 240 nm at room temperature over a 2 min time period was monitored on an Infinite M200 Pro (Tecan). The absorbance was measured at 10 different time points over this 2 minute period. Initial catalase activities were calculated by fitting experimental data to the first order kinetics as described [20] and expressed as catalase k mU/mg cell protein. The intracellular steady-state concentration of H_2O_2 was calculated from the equation: $[H_2O_2] = k_{inactivation}/k_1$, where $k_{inactivation}$ is the experimental pseudo first-order rate constant of catalase inactivation, and the value k_1 is 1.7×10^7 M^{-1} S^{-1}, the rate constant for the formation of catalase compound I in the presence of H_2O_2.

Extracellular hydrogen peroxide by Amplex Red assay

The Amplex Red Hydrogen Peroxide Assay Kit (Life Technologies) measures a catalase-sensitive signal, presumably extracellular H_2O_2. Briefly, 2.0×10^5 PC3 cells were cultured

Author Manuscript Author Manuscript Author Manuscript Author Manuscript

and 24 hours after seeding, in 4 mL of low serum media (2% fetal bovine serum), cells were incubated with the adenovirus constructs (Ad5CMVCAT, Ad5CMVSOD1 and VQAd/Empty) for 4 hours, followed by recovery in full media with 10% fetal bovine serum. After 72 hours, trypsin was used to detach cells. Cell numbers were counted and cells were reseeded in 96 well plates at a number of 5.0×10^4 cells per well. Eight hours after reseeding, the transfected cells were treated with 30 μM MnTE-2-PyP, and 16 hours later, the media were removed and the reaction mixture (1μl 5 mM Amplex Red, 1 μl 10U/ml horseradish peroxidase in 118 μl HBSS, pH 7.4) was then added to each well. Two readings were obtained immediately after adding the reaction mixture and 30 min after the 20 Gy radiation treatment respectively from each well both by an Infinite M200 Pro (Tecan) at an absorbance of 560 nm. The amount of H_2O_2 was determined by a standard curve of 0-10 μM with an equation: $[H_2O_2] = 0.0189\ x + 0.0019$, $R^2 = 0.9968$. The value of x was obtained by the subtraction of the second readings and the first readings.

ROS-GLO H_2O_2 assay

The ROS-GLO H_2O_2 Assay uses a modified luciferin substrate, based on boronate oxidation, which reacts directly with H_2O_2 to generate a luciferin precursor. Upon addition of detection reagent, precursor is converted to luciferin and Ultra-Glo™ Recombinant Luciferase included in the detection reagent produces a light signal proportional to the level of H_2O_2 in the sample. Briefly, PC3 cells were trypsinized and seeded in Nunclon 96 Flat White Plate (Thermo Fisher Scientific) with 5.0×10^4 each well. After the incubation of 30 μM MnTE-2-PyP overnight, medium was replaced with fresh complete medium. Before the 20 Gy radiation treatment, 20μl of a mixture of H_2O_2 substrate and H_2O_2 dilution buffer was immediately added to each well. Six hours after radiation, 100 μl ROS-GLO™ Detection Solution was added to each well and all samples were incubated at room temperature for 20 minutes. Luminescence was read by Infinite M200 Pro Plate Reader (Tecan) using an integration time of 1000 ms.

Nuclear Peroxy Emerald 1 (NucPE1) assay

Assays using nuclear-localized fluorescent probe for H_2O_2, NucPE1, were performed as described previously [21]. Briefly, 5.0×10^4 PC3 cells with or without 200 MOI adenovirus constructs transfection (Ad5CMVCAT or VQAd/Empty) were trypsinized and seeded on a Nunclon 96 Flat Black Plate (Thermo Fisher Scientific). After incubation with 30 μM MnTE-2-PyP or PBS overnight, the cells were then exposed to 20 Gy of radiation. One hour later, 5 μM NucPE1 was loaded to the cells for 15 minutes. After washing with PBS, PC3 cells were incubated 20 minutes in PBS with or without 100 μM H_2O_2 (for positive control). For imaging the cells, 1 μM Hoechst was also loaded to the cells with 5 μM NucPE1. The cells were photographed by using a Leica DMI 6000B microscope (Leica, Germany). Images were selected from six random microscopic fields. Fluorescence intensity quantifications were performed in ImageJ software. In brief, we used the thresholding tool to find the border of the nucleus in the Hoechst channel and these borders were selected as regions of interest (ROIs). The ROIs were overlaid on the NucPE1 image and the integrated density was measured. The distribution of integrated densities were plotted and statistical descriptions were calculated using GraphPad Prism software. This optical density analysis represents the relative level of nuclear H_2O_2 per cell.

Author Manuscript Author Manuscript Author Manuscript Author Manuscript

Detection of thiol oxidation

Determination and quantification of thiol oxidation was performed as described previously [22]. Briefly, 5.0×10^6 cells with or without transfection with Ad5CMVCAT or VQAd/Empty, were treated with MnTE-2-PyP (30 μM) or PBS overnight, then collected and centrifuged at 450 g for 5 minutes. Cell pellets were resuspended in 200 μl of lysis buffer containing 120 mM NaCl, 50 mM Tris-HCl, 5 mM EDTA, 1% NP-40 and complete protease inhibitor cocktail tablets (1 tablet/ 50 mL). The concentration of lysates were measured by a Bradford assay (Amresco) and the final concentrations were normalized to 1 mg/ml. Some of the lysates were treated with DTT (1 mM) or diamide (1 mM) for 30 minutes at room temperature (RT). Proteins (100 μg) were taken out from each sample and incubated with a solution containing 900 ul PBS, 0.1%SDS and 50 μM N- (Biotinoyl) - N'- (Iodoacetyl) Ethylenediamine (BIAM) in the dark for 30 minutes at RT. The reaction was terminated by the addition of 50 μl of 500 mM β-mercaptoethanol for 5 minutes. Streptavidin-agarose (100 μl) (Thermo Fisher Scientific) was then incubated with samples for 1 hour at RT. The streptavidin-agarose-bound complex was washed 4 times by the addition of 1 mL binding buffer (PBS+0.1%SDS) and centrifuged at 2,000 rpm. Then, each sample was boiled at 75°C for 10 minutes and western blot analysis was carried out by probing with antibodies against CREB (millipore) (1:10000), anti-HIF-1α (BD Biosciences) (1:500), HIF-1β/ARNT (Cell Signaling) (1:1000) or streptavidin-HRP (Thermo Scientific) (1:10000).

Statistical analysis

All experiments were conducted independently three or more times. Statistical analyses were performed using GraphPad Prism 6 Software version 6.0.5 for windows. Data are expressed as the mean ± standard deviation (SD). The statistical significance between different groups was evaluated with ANOVA followed by Student's *t*-test, and a $p \leq 0.05$ was considered statistically significant.

RESULTS

Human PC3 cells can be efficiently transfected with adenovirus constructs

To identify the optimal protein expression of SOD1 and catalase adenovirus vectors, PC3 cells were collected at 0, 24, 48, 72 and 96 hours post-infection and western blots were then performed for SOD1 and catalase proteins. We observed at 72 hours post-infection, that the protein expression of SOD1 and catalase peaked (data not shown). Complementarily, to determine the optimal adenovirus dose in our experiment, 0, 50, 100, 150, 200 MOI adenovirus constructs (Ad5CMVCAT, Ad5CMVSOD1 and VQAd/Empty) were used to transfect the PC3 cells followed by western blot at 72 hours post-infection. As expected, SOD1 and catalase levels increased in a dose-dependent fashion. At 200 MOI, significant increases in both SOD1 and catalase protein levels were clearly evident, whereas control virus (VQAd/Empty) had no effect (data not shown).

Furthermore, no obvious toxic effects were detected by using microscopic examination of 200 MOI transfected cells. Thus, the time point of 72 hours post-infection with 200 MOI adenovirus was used as our optimized parameters in this study. These results above suggest that human PC3 cells can be efficiently transfected with different adenovirus constructs.

Author Manuscript Author Manuscript Author Manuscript Author Manuscript

Although, SOD1 appears to be more efficiently expressed in the nucleus than catalase in PC3 cells using the viral vector infection systems.

Recombinant adenovirally expressed SOD1 and catalase localize not only to the cytoplasm, but also to the nucleus in PC3 cells

It has previously been shown that MnTE-2-PyP localizes to the nucleus and mitochondria at higher concentrations than the cytoplasm [23]. Since a goal of this study was to discern if MnTE-2-PyP was working as a SOD mimetic, we wanted to develop a model where SOD1 and catalase could be expressed in the nucleus and cytoplasm. As shown in Fig. 1A and Fig. 1B by western blot, ectopic expression of SOD1 and catalase were increased in a dose-dependent fashion not only in the cytoplasmic fraction, but also in the nuclear fraction. To this end, we performed immunofluorescence localization studies on PC3 cells following infection with either Ad5CMVSOD1 or Ad5CMVCAT. In these studies, expression of human SOD1 in PC3 cells demonstrated localization to both nuclear and cytoplasmic compartments (Fig. 1C). In addition, adenovirally expressed human catalase was also detected in the nucleus and in the perinuclear region of the cell (Fig. 1D). These results demonstrate that Ad5CMVSOD1 and Ad5CMVCAT can express their respective transgenes in the nuclear compartments. Hence, these overexpression systems can be used to discern the mechanisms by which nuclear antioxidants control gene transcription in prostate cancer cells.

Transfection of adenovirus constructs produced a significant increase in active SOD1 or catalase proteins

To determine if the SOD1 and catalase proteins produced were active, cell extracts were separated on a non-denaturing 10% polyacrylamide gel. As shown in Fig. 2A and Fig. 2B, transfection of human PC3 cells with 200 MOI resulted in a significant increase in SOD1 activity as compared with an MOI of 100. Similarly, for catalase activity, as evident in Fig. 2C and Fig. 2D, a MOI-dependent increased catalase activity was observed in human PC3 cells. PC3 cells infected with 200 MOI had significantly more catalase activity as compared to the 100 MOI group. Cells exposed to VQAd/Empty adenovirus, showed no increase in enzymatic activity for either protein. Thus, the adenoviral system is producing both active SOD1 and catalase proteins in PC3 cells, respectively.

Hydrogen peroxide is the major mediator for the suppression of human PAI-1 gene expression by MnTE-2-PyP

We have previously published that MnTE-2-PyP suppresses PAI-1 expression regulated by the p300/HIF-1β and/or CREB complex with or without 20 Gy irradiation [13]. Because we wanted to determine changes right after irradiation, we used a radiation dose of 20 Gy to aid in observing larger differences between the unirradiated and irradiated cells. To explore the gene regulation with more clinically relevant dose of irradiation, we treated the cells using 5 Gy instead of 20 Gy, and found that MnTE-2-PyP inhibited PAI-1 gene expression with 5 Gy as well as 20 Gy (Fig. 3A). Thus, similar effects were observed at 5 or 20Gy of irradiation.

Author Manuscript Author Manuscript Author Manuscript Author Manuscript

In order to determine if MnTE-2-PyP is acting solely as a SOD mimetic, we performed real-time PCR for PAI-1 gene in PC3 cells transfected with Ad5CMVSOD1. As shown in Fig. 3B, just like MnTE-2-PyP, SOD1 transfection also suppressed human PAI-1 gene expression with or without 20 Gy irradiation, as compared with empty vector transfected control cells. On the other hand, catalase overexpression in PC3 cells attenuated the inhibition of PAI-1 gene by MnTE-2-PyP with or without irradiation (Figure 3B).

We have also previously shown that MnTE-2-PyP reduces p300 binding to the HRE binding site on the PAI-1 promoter [13]. We performed a p300 ChIP-qPCR assay to test the binding of the p300 complex to the identified PAI-1 gene promoter region. As shown in Fig. 3C, a significant decrease in association of p300 with the HRE motif of PAI-1 gene promoter region was detected in PC3 cells transfected with SOD1 with or without irradiation, similarly to the results observed with MnTE-2-PyP treatment. In contrast, overexpression of catalase completely abolishes the ability of MnTE-2-PyP to inhibit the p300 complex binding to the DNA. Moreover, we performed the p300 ChIP assay on PAI-1 promoter region with different concentration of MnTE-2-PyP (1 μM, 10 μM and 30 μM), and we found that MnTE-2-PyP suppressed p300 transcriptional complex binding to DNA in a dose-dependent manner (Fig. 3D).

SOD1 enzyme and MnTE-2-PyP can catalyze the dismutation of superoxide into oxygen and H_2O_2, and catalase scavenges H_2O_2 to oxygen and water. Thus, the fact that p300 binding in MnTE-2-PyP treated cells can be reversed with catalase suggest that H_2O_2 is likely the mediator through which MnTE-2-PyP inhibits the expression of PAI-1 in PC3 cells.

In the meantime, to identify the effect of SOD1 and catalase overexpression on cell growth in the presence or the absence of MnTE-2-PyP treatment, we performed a clonogenic assay in human PC3 cells and found that SOD1 overexpression inhibited PC3 cell growth, similar to what we have observed with MnTE-2-PyP treatment [13]. Ectopic catalase also significantly suppressed cell growth, indicating that H_2O_2 removal by itself inhibits PC3 cell growth. Moreover, combination with MnTE-2-PyP also resulted in a further decrease of the PC3 colonies. Therefore, the catalase can modulate the biological behavior of PC3 cells through other signal pathways (data not shown) and MnTE-2-PyP is likely inhibiting PC3 growth by several mechanisms and not solely by inhibiting p300 signaling.

MnTE-2-PyP treatment and SOD1 overexpression enhances intracellular hydrogen peroxide levels

We then focused on the changes of intracellular and extracellular H_2O_2 levels after transfection with SOD1, catalase or treatment with MnTE-2-PyP. The intracellular steady-state levels of H_2O_2 were estimated using a sensitive assay based on 3-aminotriazole inhibition of catalase [19]. PC3 cells overexpressing SOD1, catalase or treatment with MnTE-2-PyP were incubated with 0 or 20 mM 3-aminotriazole for different time intervals to determine steady-state intracellular H_2O_2 concentrations. As shown in Fig. 4A, there was a significant increase in the steady-state level of intracellular H_2O_2 after SOD1 transfection or MnTE-2-PyP treatment with or without 20 Gy irradiation. As expected, ectopic catalase profoundly attenuated the intracellular H_2O_2 steady state levels produced by MnTE-2-PyP.

Author Manuscript Author Manuscript Author Manuscript Author Manuscript

Furthermore, to confirm the effect of MnTE-2-PyP on the production of H_2O_2 levels inside the cells, we measured H_2O_2 levels using a ROS-GLO probe (Promega). This probe measures both intra and extracellular H_2O_2. Consistent with the data we obtained above, increased H_2O_2 levels were clearly observed following MnTE-2-PyP treatment with or without 20 Gy radiation in human PC3 cells (Fig. 4B). Moreover, we also performed the ROS-GLO assay on PC3 cells treated with different concentration of MnTE-2-PyP (1 μM, 10 μM and 30 μM), and we found that MnTE-2-PyP enhanced the levels of intra and extracellular H_2O_2 in a dose-dependent manner (Fig. 4C).

We next determined if extracellular H_2O_2 could be altered respectively in the media of cells after SOD1 and catalase transfection with or without MnTE-2-PyP treatment using the Amplex Red Hydrogen Peroxide Assay. Any H_2O_2 produced intracellularly that diffuses out of the cells or produced locally at the plasma membrane would be detected by using this assay. However, as shown in Fig. 4D, no evidence of changes in extracellular H_2O_2 was detected in PC3 cells after transfection with either SOD1, catalase adenovirus or treatment with MnTE-2-PyP.

Because we were interested in the nucleus, we wanted to determine if this increased intracellular H_2O_2 was occurring in the nuclear compartment. NucPE1 has been previously shown to be a nuclear-localized fluorescent probe for H_2O_2, and it can directly and specifically measure nuclear H_2O_2 concentration [21]. As is shown in Fig. 5A, there was a significant increase in the levels of nuclear H_2O_2 concentration after MnTE-2-PyP treatment. Additionally, when catalase overexpressing cells were treated with MnTE-2-PyP, the H_2O_2 concentration detected by NucPE1 was significantly diminished with or without irradiation (Fig. 5B). This data is further confirmation that MnTE-2-PyP is producing high levels of H_2O_2 in the nucleus and that the catalase over-expressing system can scavenge this nuclear H_2O_2.

MnTE-2-PyP enhances H_2O_2-mediated protein oxidation

In order to determine whether these high levels of H_2O_2 observed in MnTE-2-PyP result in thiol oxidation of proteins, we used a BIAM assay to determine oxidation status of thiol groups in the PC3 cell lysates [22]. BIAM will bind to reduced thiol groups, but not oxidized thiols and streptavidin beads were used to immunoprecipate these proteins from the overall cell lysate. From Fig. 6A, it is clear that the amount of overall proteins that were bound to BIAM in MnTE-2-PyP group was reduced as compared with the non-treated cells, which indicates that these thiols were oxidized in the presence of MnTE-2-PyP. DTT, a reducing agent, and diamide, a strong oxidizing agent were added for internal controls for the BIAM assay. We also explored if ectopic catalase could inhibit thiol groups oxidation by MnTE-2-PyP. As shown in Fig. 6B, although ectopic catalase alone did not change thiol oxidation levels in PC3 cells without treatment of MnTE-2-PyP, catalase overexpression clearly reversed the thiol oxidation by MnTE-2-PyP as compared with empty vector transfected group, indicating that MnTE-2-PyP thiol oxidation was mediated by H_2O_2.

Furthermore, to determine specifically which proteins are oxidized in the presence of MnTE-2-PyP, we performed the BIAM assay followed by western blotting for p300. As shown in Fig. 6C, p300 was oxidized in the presence of MnTE-2-PyP or diamide, similar to

Author Manuscript Author Manuscript Author Manuscript Author Manuscript

the trend observed in Fig. 6A. Then we used densitometric analysis to quantify these changes. As shown in Fig. 6D, MnTE-2-PyP significantly oxidized thiol groups present on the p300 protein, similar to the oxidation of p300 in the presence of diamide. We have previously shown that MnTE-2-PyP treatment does not affect overall p300 protein expression levels [13], so this loss in protein detected by the BIAM assay is most likely due to the oxidation of thiols of the p300 protein. We tried to measure other transcription factors associated with the p300 transcriptional complex (i.e., HIF-1α, HIF-1β and CREB), but we could not detect these proteins via this method (data not shown).

DISCUSSION

It has been previously reported by our laboratory that MnTE-2-PyP reduces prostate cancer growth and metastasis [13]. We found that MnTE-2-PyP inhibits the binding of p300/HIF-1/CREB transcriptional complex to the promoter region of PAI-1 gene, reduces histone acetylation, and consequently, significantly suppresses the expression of human PAI-1 gene [13]. However, the underlying mechanism(s) as to how MnTE-2-PyP reduces p300 association binding to DNA has not been elucidated. In this current study, by developing a model where SOD1 and catalase are expressed in the nucleus, we found that SOD1 overexpression results in similar activity observed in MnTE-2-PyP treated cells. Conversely, overexpression of catalase reverses MnTE-2-PyP activity. These data suggest that H_2O_2 is likely the mediator through which MnTE-2-PyP inhibits PAI-1 expression. In accordance with this idea, MnTE-2-PyP was found to cause a significant increase in intracellular H_2O_2 concentrations, which resulted in the oxidation of p300. We speculate that p300 oxidation inhibits binding of the p300/HIF-1/CREB complex to the promoter region of PAI-1 gene. This is the first study to directly measure H_2O_2 levels in MnTE-2-PyP treated cells. We showed that MnTE-2-PyP, alone or in combination with radiation, creates a significant increase in intracellular H_2O_2 levels, specifically in the nucleus. We speculate that this increased nuclear H_2O_2 mediates the thiol oxidation and that this could be an important mechanism by which MnTE-2-PyP works as an anti-tumor agent. However, since catalase overexpression in MnTE-2-PyP treated cells also resulted in significant growth inhibition, inhibition of p300 signaling is likely not the only mechanism by which MnTE-2-PyP is inhibiting PC3 cell growth.

Redox-active manganese porphyrins, such as MnTE-2-PyP, have been developed with characteristics that mimic the active center of naturally occurring metalloenzymes, which catalytically breakdown superoxide and inhibit peroxynitrite formation. Regarding its ability to scavenge superoxide into H_2O_2 and oxygen, it acts as an SOD mimetic. However, previous research indicates that the SOD activity of MnTE-2-PyP is just one of its many activities with potential biological effects. MnTE-2-PyP has been shown to alter transcription factor binding, which results in the alteration of major signaling pathways. It is unclear if this change in signaling is a result of changing the redox environment or a redox-independent mechanism.

Generally speaking, the oxidation state of the manganese at the center of the metalloporphyrins have four varied forms: Mn (II), Mn (III), O=Mn (IV) and O=Mn (V) [24]. And the oxidation state of Mn (III) is most stable among those conditions. When

Author Manuscript Author Manuscript Author Manuscript Author Manuscript

MnTE-2-PyP functions as a SOD mimetic, it usually alters reduction and oxidation reactions between redox states of Mn (II) and Mn (III). Besides, MnTE-2-PyP can also use several reducing agents to cycle during this oxidation shift of Mn (II) and Mn (III) states, resulting in the production of H_2O_2. Tovmasyan *et al.* have showed that MnTE-2-PyP switches between the oxidation states of Mn (II) and Mn (III) in the presence of reducing agent ascorbate, which generates a burst of H_2O_2 [25]. Furthermore, when the environment is more oxidizing, the manganese localized in the center of MnTE-2-PyP, can be oxidized to O=Mn (IV) or O=Mn (V). During these conditions, such as treatment with chemotherapy, MnTE-2-PyP is highly oxidizing. Jaramillo *et al.* showed that in the presence of dexamethasone treatment, MnTE-2-PyP S-glutathionylates the cysteines of NF-κB (Nuclear Factor-kappa B) subunits p65, which prevents NF-κB binding and its transcriptional activity [26]. In a previous study this same group showed that MnTE-2-PyP in combination with dexamethasone, but not alone, creates H_2O_2 which induces apoptosis in lymphoma cells [27]. We found that MnTE-2-PyP alone and in combination with radiation enhanced H_2O_2 signaling, thus, MnTE-2-PyP may produce different amounts of H_2O_2 in different cell types. Ascorbate levels in MnTE-2-PyP treated PC3 cells may contribute to H_2O_2 production as well, this has not yet been investigated. In addition, the impacts of MnTE-2-PyP on several transcription factors HIF-1α, SP-1 and AP-1 have also been explored [28-30]. Therefore, MnTE-2-PyP has been regarded as a redox regulator of cellular transcriptional activities rather than solely as a SOD mimetic. In our study, we found that even without chemotherapy or radiotherapy treatment, MnTE-2-PyP is reactive towards protein thiols. However, we do not believe that this oxidation is direct. We postulate that by dismuting superoxide, MnTE-2-PyP creates localized elevated H_2O_2 levels, which affects signaling through induced H_2O_2 mediated cysteines oxidation of target proteins.

We acknowledge that there are controversies in the field that SOD is capable of producing large amounts of H_2O_2. In theory, superoxide, if left alone, will dismute to H_2O_2 on its own, albeit at a slower rate than in the presence of SOD [31]. Therefore, increased SOD activity should not result in overall higher H_2O_2 concentrations. However, our study and other studies have shown that SOD overexpression results in increased steady state H_2O_2 levels. In this study we also show that the SOD mimetic, MnTE-2-PyP, is acting in a similar manner [32, 33]. One plausible explanation could be that in a cell, superoxide interacts with other cellular molecules, such as nitric oxide and, therefore, H_2O_2 production is blunted. When SOD levels are increased, more superoxide is directly scavenged, which leads to increased H_2O_2 concentrations. The PC3 cancer cells are highly metabolic and have dysfunctional mitochondria, so we postulate that electrons from these damaged mitochondria are being effectively scavenged by SOD overexpression and by MnTE-2-PyP treatment.

H_2O_2 is a very important molecule in the regulation of a wide variety of biological processes. Depending on its location and concentration, it can serve both beneficial and harmful roles within the cells. However, the methods to quantify and track the small, diffusible H_2O_2 molecules with spatial and temporal fidelity in live cells still remain limited [34, 35]. In this paper, we carried out four different assays to measure the concentration levels of H_2O_2 after we treated PC3 cells with or without MnTE-2-PyP: 3-aminotriazole inhibition of catalase assay, ROS-GLO assay, NucPE1 assay, and Amplex Red Hydrogen Peroxide Assay. To our knowledge, this is the first study to directly measure the H_2O_2 levels

Author Manuscript Author Manuscript Author Manuscript Author Manuscript

induced by MnTE-2-PyP alone inside or outside the cells. We performed a sensitive method for the measurement of intracellular H_2O_2 based on irreversible inhibition of catalase by 3-aminotriazole [17, 18]. The extent of 3-aminotriazole mediated catalase inhibition is dependent on the initial steady-state levels of intracellular H_2O_2, so the rate of inhibition can be used to estimate H_2O_2 concentration inside the cells. A significant increase (more than 2 fold) of intracellular H_2O_2 was also detected by this assay following with MnTE-2-PyP treatment with or without radiation treatment. Using the ROS-GLO H_2O_2 assay, which is regarded as a homogeneous, rapid and sensitive luminescent assay to measure both intra and extracellular H_2O_2, we were also able to detect a 2 fold increase of H_2O_2 levels after human prostate cancer cells were exposed to MnTE-2-PyP with or without 20 Gy irradiation. As the ROS-GLO H_2O_2 assay does not rely on a reaction catalyzed by horseradish peroxidase, it is a direct assay to detect H_2O_2 levels, results in a much lower false detection rate.

Radiation has been shown to increase NOX4 activity and NOX4 is located in cell membranes and found in the nucleus. NOX4 is likely a major of superoxide and hydrogen peroxide in the nucleus after irradiation [36-38]. Although, there is controversy in the field as to whether NOX4 makes superoxide or only hydrogen peroxide, we did not investigate which ROS species was produced by NOX4 in our system. Due to this fact, the source of ROS from the mitochondria could also contribute to the superoxide radical anion being produced with irradiation and the hydrogen peroxide could also diffuse into the nucleus. MnTE-2-PyP localizes to both the mitochondria and the nucleus and could scavenge superoxide in both of these compartments. Since we know that MnTE-2-PyP diffuses to the nucleus and we have detected aberrant transcription factor activity and binding following MnTE-2-PyP treatment, we wanted to determine if this increased intracellular H_2O_2 was occurring in the nuclear compartment. Therefore, we used a nuclear-localized fluorescent probe for H_2O_2, NucPE1, to selectively measure H_2O_2 fluxes in the nucleus [21]. A significant increase in nuclear H_2O_2 was clearly detected in cells treated with MnTE-2-PyP alone or in combination with radiation. Thus, by using these variety of methods for H_2O_2 detection, we can draw this conclusion: MnTE-2-PyP treatment enhances intracellular H_2O_2 levels, specifically in the nucleus in PC3 cells.

H_2O_2 generation is a normal physiologic process in the cells and any H_2O_2 produced intracellularly can diffuse readily out of the cells. In this study, we performed an Amplex Red Hydrogen Peroxide Assay to detect H_2O_2 in the medium. Since the indicator enters the cells poorly, this method measures only extracellular H_2O_2 concentration. However, we found MnTE-2-PyP had no effect on extracellular H_2O_2 levels. This phenomenon may be explained by the following possibilities. First, the Amplex Red Hydrogen Peroxide Assay may not be sensitive enough to detect the alterations in extracellular levels. The intracellular levels of H_2O_2 may not be sufficient to raise extracellular H_2O_2 concentration, which is necessary for its detection by this assay. Second, H_2O_2 may react with intracellular sinks before it can leave the cells. Third, we only measured 1 hour after radiation, more time may be needed to observe the accumulation of extracellular H_2O_2. Finally, another possibility is that the cell medium may be interfering with this assay.

A wide range of cellular biological processes, such as cell signaling and gene transcription, are redox regulated. H_2O_2 is known as a critical molecule that is involved in redox

Author Manuscript Author Manuscript Author Manuscript Author Manuscript

regulation and is very reactive towards cysteine (Cys) residues [39]. Through the reversible oxidation of specific cysteine residues, H_2O_2 can translate the redox state into a signal that ultimately leads to an appropriate cellular response. Generally speaking, low levels of H_2O_2 can oxidize the Cys thiol initially to sulfenic acid (SOH). This is a very reactive species; it will rapidly form a disulfide bond or a sulfenamide if there is any thiol available in the vicinity, which results in intermediate conformational changes within proteins or protein complexes. On the other hand, with larger doses of H_2O_2, SOH may become further oxidized to sulfinic (SO_2H) or sulfonic (SO_3H) acid. The oxidation towards sulfonic acid is seen as to be an irreversible stage, and a fully oxidized cysteine residue is, therefore, frequently referred to as being over or hyper oxidized. Glutathionylation and S-nitrosylation can also modify cysteine residues as well. It is unclear which type of oxidation is taking place in the PC3 cells treated with MnTE-2-PyP.

Cys residues in proteins can act as sensors of H_2O_2, providing cells with a mechanism for sensing and responding to changes in the redox environment [40]. The reversibility of some of these oxidative protein modifications makes them ideally suited to take on regulatory roles in protein function. This is especially true for disulfide bond formation, which has the potential to mediate extensive yet fully reversible structural and functional changes, rapidly adjusting the protein's activity to the prevailing oxidant levels [41]. H_2O_2 sensors, including some transcription factor and transcriptional coactivators contain exposed and reactive cysteine residues. Transcription factors, CREB and HIF-1, alter many signaling pathways in cells, and contribute to cancer progression by regulating key genes expression, which associate with cell proliferation, invasion, and angiogenesis. Some studies have shown that CREB and HIF-1 are both redox-sensitive primarily through cysteine residues present in DNA binding domain [42, 43]. In addition, the co-activator p300, which promotes transcription by connecting transcription factors to the basal transcriptional machinery, is also reported to contain cysteine residues in its functional domain [44]. In order to determine which transcription factor or co-activator is been oxidized by MnTE-2-PyP, a protein oxidation experiment was performed. Although target proteins CREB, HIF-1α, and HIF-1β were not detected by this assay, p300 was clearly oxidized by MnTE-2-PyP. We speculate that CREB and HIF proteins are present at too low of concentrations to detect by this methodology.

p300 is a 300 kDa protein, which has different functional domains: a histone acetyltransferase (HAT) domain, a bromodomain, a KIX domain, a C-terminal glutamine-rich domain and three cysteine-histidine rich domains (CH1, CH2, CH3). All of these above functional domains enable p300 to act as a powerful adaptor molecule interacting with a wide array of transcription factors and co-factors [45]. CH1, CH2 and CH3 are all homologous Zn^{2+} binding domains of p300 containing numerous cysteine and histidine residues [46]. With few exceptions, the CH1 and CH3 domains bind different sets of transcription factors despite their predicted structural similarity, but CH2 region is structurally unrelated to the CH1 and CH3 domains [46]. From this study, it is clear that oxidation of p300 by MnTE-2-PyP could result in reduced binding of p300 transcriptional complex to the promoter region of PAI-1 gene. But we still do not know which domains of p300 might be oxidized. Cysteine-histidine rich domains CH1 and CH3 have been shown to be very important for interaction with transcription factor p53, HIF-1 [44, 47]. However, we

Author Manuscript Author Manuscript Author Manuscript Author Manuscript

have previously shown that MnTE-2-PyP treatment does not interfere the binding between p300 and CREB/HIF-1 transcription factors [13], so it is not likely to be oxidized in these domains. The p300 CH2 region has been predicted to contain a plant homeodomain (PHD) and Ragvin *et al.* have shown that the CH2 region is required for chromatin binding [48]. Therefore, we postulate that MnTE-2-PyP may be oxidizing p300 in CH2 domains, and cause a conformational change resulting in reduced binding of transcriptional complex to DNA, which is consistent with our previous data [1313]. However, more experiments need to be done to prove this hypothesis.

In summary, we have shown that MnTE-2-PyP treatment induces redox effects, which can be mimicked by SOD1 overexpression. Furthermore, we show that catalase overexpression blocks the ability of MnTE-2-PyP to oxidize thiols. This is the first study to directly measure H_2O_2 levels after MnTE-2-PyP treatment, indicating that MnTE-2-PyP alone produces high levels of H_2O_2, specifically in the nucleus. Most importantly, this study advances our understanding of redox regulation for manganese porphyrins. In this paper, MnTE-2-PyP has been found to function as a redox regulator through post-translational modification of critical proteins at cysteine thiols. These studies are crucial in determining how MnTE-2-PyP regulates redox signaling and alters the behavior of cancer cells. Understanding how MnTE-2-PyP works can lead to the development for the treatment of prostate cancer.

ACKNOWLEDGMENTS

This work was supported by National Institutes of Health Grants 1R01CA178888 (ROD), by the National Natural Science Foundation of China No. 81172186 (QT) and by the Fred and Pamela Buffet Cancer Center Support Grant P30CA036727 (ROD).

We would like to thank Dr. Christopher Chang from the University of California at Berkley for providing the NucPE1 construct to use for this study.

The abbreviations used are

PAI-1	Plasminogen activator inhibitor-1
ROS	Reactive oxygen species
HRE	Hypoxia-response element
SOD1	Superoxide dismutase 1
HIF-1	Hypoxia-inducible factor-1
CREB	cAMP response element-binding protein
ChIP	Chromatin immunoprecipitation
ARNT	Aryl hydrocarbon receptor nuclear translocator
CAT	catalase
NucPE1	Nuclear peroxy emerald 1

Author Manuscript Author Manuscript Author Manuscript Author Manuscript

REFERENCES

[1]. Siegel R, Naishadham D, Jemal A. Cancer statistics, 2012. CA: a cancer journal for clinicians. 2012; 62:10–29. [PubMed: 22237781]

[2]. Cooperberg MR, Broering JM, Carroll PR. Time trends and local variation in primary treatment of localized prostate cancer. Journal of clinical oncology: official journal of the American Society of Clinical Oncology. 2010; 28:1117–1123. [PubMed: 20124165]

[3]. Elliott SP, Malaeb BS. Long-term urinary adverse effects of pelvic radiotherapy. World journal of urology. 2011; 29:35–41. [PubMed: 20959990]

[4]. Sullivan L, Williams SG, Tai KH, Foroudi F, Cleeve L, Duchesne GM. Urethral stricture following high dose rate brachytherapy for prostate cancer. Radiotherapy and oncology: journal of the European Society for Therapeutic Radiology and Oncology. 2009; 91:232–236. [PubMed: 19097660]

[5]. Moding EJ, K. M, Kirsch DG. Strategies for optimizing the response of cancer and normal tissues to radiation. Nat Rev Drug Discov. 2013; 12:526–542. [PubMed: 23812271]

[6]. Kouvaris JR, K. V, Vlahos LJ. Amifostine: the first selective-target and broad-spectrum radioprotector. Oncologist. 2007; 12:738–747. [PubMed: 17602063]

[7]. Hensley ML, H. K, Kewalramani T, Green DM, Meropol NJ, Wasserman TH, Cohen GI, Emami B, Gradishar WJ, Mitchell RB, Thigpen JT, Trotti A 3rd, von Hoff D, Schuchter LM. American Society of Clinical Oncology 2008 clinical practice guideline update: use of chemotherapy and radiation therapy protectants. J Clin Oncol. 2009; 27:127–145. [PubMed: 19018081]

[8]. Cassatt DR, F. C, Bachy CM, Hanson MS. Preclinical modeling of improved amifostine (Ethyol) use in radiation therapy. Semin Radiat Oncol. 2002; 12:97–102. [PubMed: 11917293]

[9]. Cassatt DR, F. C, Kifle G, Bachy CM. Preclinical studies on the radioprotective efficacy and pharmacokinetics of subcutaneously administered amifostine. Semin Oncol. 2002; 29:2–8.

[10]. Oberley-Deegan RE, Lee YM, Morey GE, Cook DM, Chan ED, Crapo JD. The antioxidant mimetic, MnTE-2-PyP, reduces intracellular growth of Mycobacterium abscessus. American journal of respiratory cell and molecular biology. 2009; 41:170–178. [PubMed: 19097985]

[11]. Oberley-Deegan RE, Steffan JJ, Rove KO, Pate KM, Weaver MW, Spasojevic I, Frederick B, Raben D, Meacham RB, Crapo JD, Koul HK. The antioxidant, MnTE-2-PyP, prevents side-effects incurred by prostate cancer irradiation. PloS one. 2012; 7:e44178. [PubMed: 22984473]

[12]. Rabbani ZN, Spasojevic I, Zhang X, Moeller BJ, Haberle S, Vasquez-Vivar J, Dewhirst MW, Vujaskovic Z, Batinic-Haberle I. Antiangiogenic action of redox-modulating Mn(III) meso-tetrakis(N-ethylpyridinium-2-yl)porphyrin, MnTE-2-PyP(5+), via suppression of oxidative stress in a mouse model of breast tumor. Free radical biology & medicine. 2009; 47:992–1004. [PubMed: 19591920]

[13]. Tong Q, W. M, Kosmacek EA, O'Connor BP, Harmacek L, Venkataraman S, Oberley-Deegan RE. MnTE-2-PyP reduces prostate cancer growth and metastasis by suppressing p300 activity and p300/HIF-1/CREB binding to the promoter region of the PAI-1 gene. Free radical biology & medicine. 2016; 94:185–194. [PubMed: 26944191]

[14]. Carter AB, T. L, Venkataraman S, Oberley LW, Zhang Y, Buettner GR, Spitz DR, Hunninghake GW. High levels of catalase and glutathione peroxidase activity dampen H2O2 signaling in human alveolar macrophages. American journal of respiratory cell and molecular biology. 2004; 31:43–53. [PubMed: 14962975]

[15]. Weydert CJ, C. J. Measurement of superoxide dismutase, catalase and glutathione peroxidase in cultured cells and tissue. Nature protocols. 2010; 5:51–66. [PubMed: 20057381]

[16]. Das PM, Ramachandran K, vanWert J, Singal R. Chromatin immunoprecipitation assay. BioTechniques. 2004; 37:961–969. [PubMed: 15597545]

[17]. Royall JA, G. P, Parks DA, Freeman BA. Responses of vascular endothelial oxidant metabolism to lipopolysaccharide and tumor necrosis factor-alpha. Arch Biochem Biophys. 1992; 294:686–694. [PubMed: 1567224]

[18]. Yusa T, B. J, Crapo JD, Freeman BA. Hyperoxia increases H2O2 production by brain in vivo. J Appl Physiol (1985). 1987; 63:353–358. [PubMed: 3624137]

Author Manuscript Author Manuscript Author Manuscript Author Manuscript

[19]. Wagner BA, E. C, Reszka KJ, Buettner GR, Burns CP. Doxorubicin increases intracellular hydrogen peroxide in PC3 prostate cancer cells. Arch Biochem Biophys. 2005; 440:181–190. [PubMed: 16054588]

[20]. H. A. Catalase in vitro. Methods Enzymol. 1984; 105:121–126. [PubMed: 6727660]

[21]. Dickinson BC, T. Y, Chang Z, Chang CJ. A nuclear-localized fluorescent hydrogen peroxide probe for monitoring sirtuin-mediated oxidative stress responses in vivo. Chem Biol. 2011; 18:943–948. [PubMed: 21867909]

[22]. Hill BG, R. C, Oh JY, Johnson MS, Landar A. Methods for the determination and quantification of the reactive thiol proteome. Free Radic Biol Med. 2009; 47:675–683. [PubMed: 19527783]

[23]. Batinic-Haberle I, S. I, Tse HM, Tovmasyan A, Rajic Z, St Clair DK, Vujaskovic Z, Dewhirst MW, Piganelli JD. Design of Mn porphyrins for treating oxidative stress injuries and their redox-based regulation of cellular transcriptional activities. Amino acids. 2012; 42:95–113. [PubMed: 20473774]

[24]. Reaney SH, K.-U. C, Smith DR. Manganese oxidation state and its implications for toxicity. Chem Res Toxicol. 2002; 15:1119–1126. [PubMed: 12230404]

[25]. Tovmasyan A, S. R, Boss MK, Bueno-Janice JC, Bader BH, Thomas M, Reboucas JS, Orr M, Chandler JD, Go YM, Jones DP, Venkatraman TN, Haberle S, Kyui N, Lascola CD, Dewhirst MW, Spasojevic I, Benov L, Batinic-Haberle I. Anticancer therapeutic potential of Mn porphyrin/ascorbate system. Free Radic Biol Med. 2015; 89:1231–1247. [PubMed: 26496207]

[26]. Jaramillo MC, B. M, Batinic-Haberle I, Tome ME. Manganese (III) meso-tetrakis N-ethylpyridinium-2-yl porphyrin acts as a pro-oxidant to inhibit electron transport chain proteins, modulate bioenergetics, and enhance the response to chemotherapy in lymphoma cells. Free radical biology & medicine. 2015; 83:89–100. [PubMed: 25725417]

[27]. Jaramillo MC, B. M, Crapo JD, Batinic-Haberle I, Tome ME. Manganese porphyrin, MnTE-2-PyP5+, Acts as a pro-oxidant to potentiate glucocorticoid-induced apoptosis in lymphoma cells. Free Radic Biol Med. 2012; 52:1272–1284. [PubMed: 22330065]

[28]. Tse HM, M. M, Piganelli JD. Mechanistic analysis of the immunomodulatory effects of a catalytic antioxidant on antigen-presenting cells: implication for their use in targeting oxidation-reduction reactions in innate immunity. Free Radic Biol Med. 2004; 36:233–247. [PubMed: 14744635]

[29]. Zhao Y, C. L, Oberley TD, Batinic-Haberle I, St Clair W, Epstein CJ, St Clair D. A mechanism-based antioxidant approach for the reduction of skin carcinogenesis. Cancer Res. 2005; 65:1401–1405. [PubMed: 15735027]

[30]. Moeller BJ, C. Y, Li CY, Dewhirst MW. Radiation activates HIF-1 to regulate vascular radiosensitivity in tumors: role of reoxygenation, free radicals, and stress granules. Cancer Cell. 2004; 5:429–441. [PubMed: 15144951]

[31]. Liochev SI, F. I. The effects of superoxide dismutase on H2O2 formation. Free Radic Biol Med. 2007; 42:1465–1469. [PubMed: 17448892]

[32]. Dasgupta J, S. S, Connor KM, Rodriguez AM, Tirosh O, Beckman JS, Jourd'Heuil D, Melendez JA. Manganese superoxide dismutase protects from TNF-alpha-induced apoptosis by increasing the steady-state production of H2O2. Antioxid Redox Signal. 2006; 8:1295–1305. [PubMed: 16910777]

[33]. Wang M, K. J, Venkataraman S, Domann FE, Zhang HJ, Schafer FQ, Flanagan SW, Weydert CJ, Spitz DR, Buettner GR, Oberley LW. Manganese superoxide dismutase suppresses hypoxic induction of hypoxia-inducible factor-1alpha and vascular endothelial growth factor. Oncogene. 2005; 24:8154–8166. [PubMed: 16170370]

[34]. Brewer TF, G. F, Onak CS, Carroll KS, Chang CJ. Chemical approaches to discovery and study of sources and targets of hydrogen peroxide redox signaling through NADPH oxidase proteins. Annu Rev Biochem. 2015; 84:765–790. [PubMed: 26034893]

[35]. Lippert AR, V. d. B. G, Chang CJ. Boronate oxidation as a bioorthogonal reaction approach for studying the chemistry of hydrogen peroxide in living systems. Acc Chem Res. 2011; 44:793–804. [PubMed: 21834525]

[36]. Kuroda J, N. K, Yamasaki T, Nakamura K, Takeya R, Kuribayashi F, Imajoh-Ohmi S, Igarashi K, Shibata Y, Sueishi K, Sumimoto H. The superoxide-producing NAD(P)H oxidase Nox4 in the

Author Manuscript Author Manuscript Author Manuscript Author Manuscript

nucleus of human vascular endothelial cells. Genes Cells. 2005; 10:1139–1151. [PubMed: 16324151]

[37]. Matsushima S, K. J, Ago T, Zhai P, Park JY, Xie LH, Tian B, Sadoshima J. Increased oxidative stress in the nucleus caused by Nox4 mediates oxidation of HDAC4 and cardiac hypertrophy. Circ Res. 2013; 112:651–663. [PubMed: 23271793]

[38]. Stanicka J, R. E, Woolley JF, Cotter TG. NADPH oxidase-generated hydrogen peroxide induces DNA damage in mutant FLT3-expressing leukemia cells. The Journal of biological chemistry. 2015; 290:9348–9361. [PubMed: 25697362]

[39]. Veal EA, D. A, Morgan BA. Hydrogen peroxide sensing and signaling. Mol Cell. 2007; 26:1–14. [PubMed: 17434122]

[40]. Chung HS, W. S, Venkatraman V, Murray CI, Van Eyk JE. Cysteine oxidative posttranslational modifications: emerging regulation in the cardiovascular system. Circ Res. 2013; 112:382–392. [PubMed: 23329793]

[41]. Putker M, V. H, Dansen TB. Intermolecular disulfide-dependent redox signalling. Biochem Soc Trans. 2014; 42:971–978. [PubMed: 25109988]

[42]. Ichiki T, Tokunou T, Fukuyama K, Iino N, Masuda S, Takeshita A. Cyclic AMP response element-binding protein mediates reactive oxygen species-induced c-fos expression. Hypertension. 2003; 42:177–183. [PubMed: 12810757]

[43]. Nikinmaa M, Pursiheimo S, Soitamo AJ. Redox state regulates HIF-1alpha and its DNA binding and phosphorylation in salmonid cells. Journal of cell science. 2004; 117:3201–3206. [PubMed: 15199099]

[44]. Gu J, M. J, Huang LE. Molecular mechanism of hypoxia-inducible factor 1alpha - p300 interaction. A leucine-rich interface regulated by a single cysteine. The Journal of biological chemistry. 2001; 276:3550–3554. [PubMed: 11063749]

[45]. Delvecchio M, G. J, Aguilar-Gurrieri C, Ortega E, Panne D. Structure of the p300 catalytic core and implications for chromatin targeting and HAT regulation. Nat Struct Mol Biol. 2013; 20:1040–1046. [PubMed: 23934153]

[46]. Freedman SJ, S. Z, Poy F, Kung AL, Livingston DM, Wagner G, Eck MJ. Structural basis for recruitment of CBP/p300 by hypoxia-inducible factor-1 alpha. Proc Natl Acad Sci U S A. 2002; 99:5367–5372. [PubMed: 11959990]

[47]. Teufel DP, F. S, Bycroft M, Fersht AR. Four domains of p300 each bind tightly to a sequence spanning both transactivation subdomains of p53. Proc Natl Acad Sci U S A. 2007; 104:7009–7014. [PubMed: 17438265]

[48]. Ragvin A, V. H, Erdal S, Arskog V, Tufteland KR, Breen K, ØYan AM, Eberharter A, Gibson TJ, Becker PB, Aasland R. Nucleosome binding by the bromodomain and PHD finger of the transcriptional cofactor p300. J Mol Biol. 2004; 337:773–788. [PubMed: 15033350]

Author Manuscript Author Manuscript Author Manuscript Author Manuscript

Highlights

- We show that MnTE-2-PyP treatment mimics the activity of Cu/ZnSOD overexpression. Furthermore, we show that catalase overexpression blocks MnTE-2-PyP activity.
- MnTE-2-PyP treatment alone produces high levels of hydrogen peroxide, specifically in the nucleus.
- MnTE-2-PyP oxidizes protein thiols and this can be reversed with catalase overexpression.
- These studies are crucial in determining how MnTE-2-PyP regulates redox signaling and alters the behavior of cancer cells. Understanding how MnTE-2-PyP works can lead to the development for the treatment of prostate cancer.

Author Manuscript
Author Manuscript
Author Manuscript
Author Manuscript

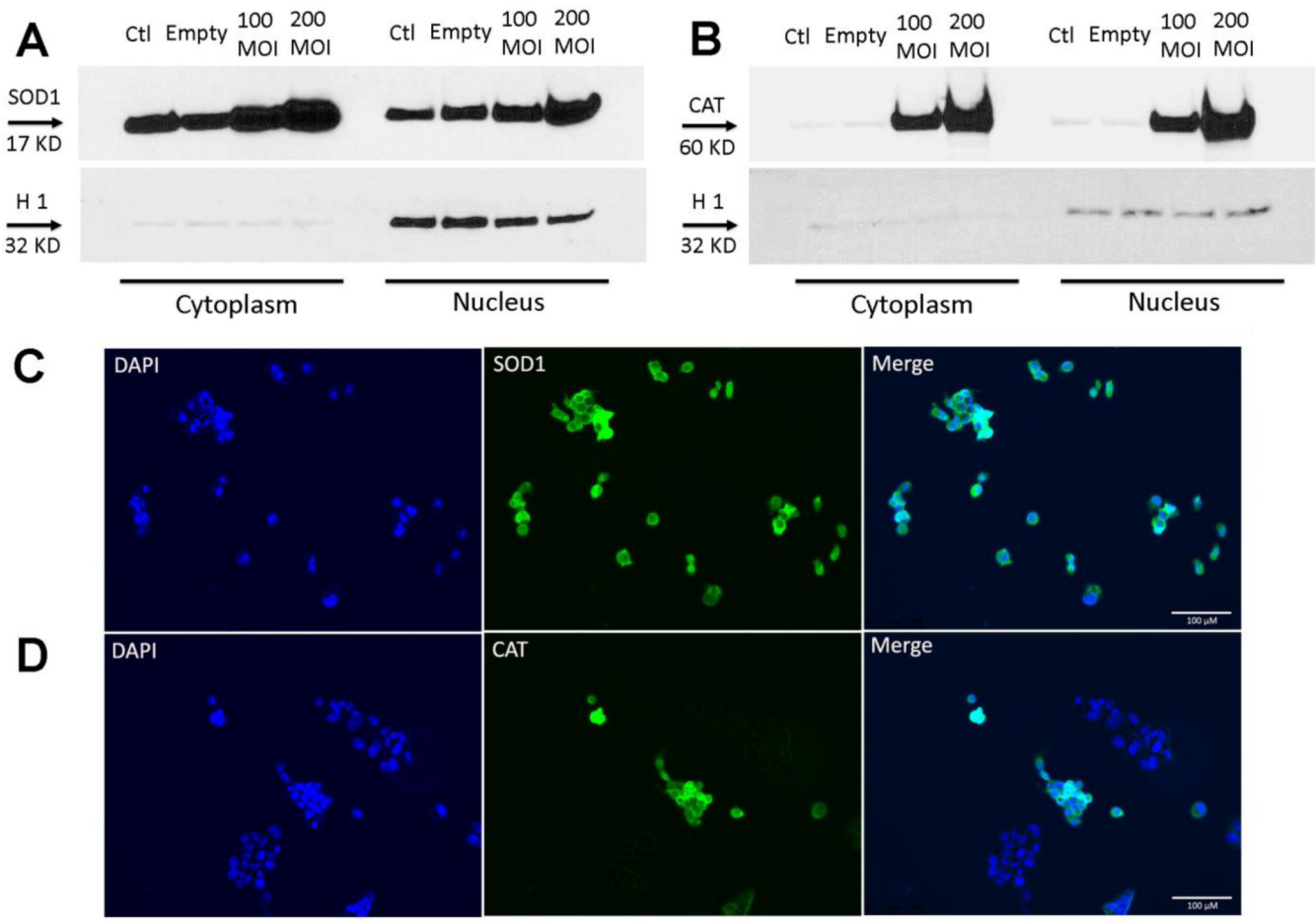

Figure 1. Expression and subcellular localization of overexpressed antioxidant proteins, SOD1 and catalase

PC3 cells treated with different MOIs of adenovirus containing SOD1 or catalase. Western blot expression in the cytoplasmic and nuclear fraction of human PC3 cells for SOD1 **(A)** or catalase **(B)**. Histone 1 was used as nuclear marker. Note: 30 μg of cytoplasmic homogenate proteins and 20 μg of nuclear homogenate proteins were used for western blotting. Subcellular localization of overexpressed SOD1 **(C)** and catalase **(D)** in infected cells. 3×10^4 PC3 cells were treated with 200 MOI Ad5CMVSOD1 or Ad5CMVCAT, and samples were subjected to immunofluorescence microscopy. (Left) DAPI was used as a marker for nuclear staining. (Middle) Immunofluorescent microscopy of SOD1 or catalase using anti-SOD1 or anti-catalase antibody. (Right) Merged images. The cells were examined by a DM4000 B LED fluorescence microscope. Scale bar is 100 μm. Representative of three separate experiments.

Author Manuscript Author Manuscript Author Manuscript Author Manuscript

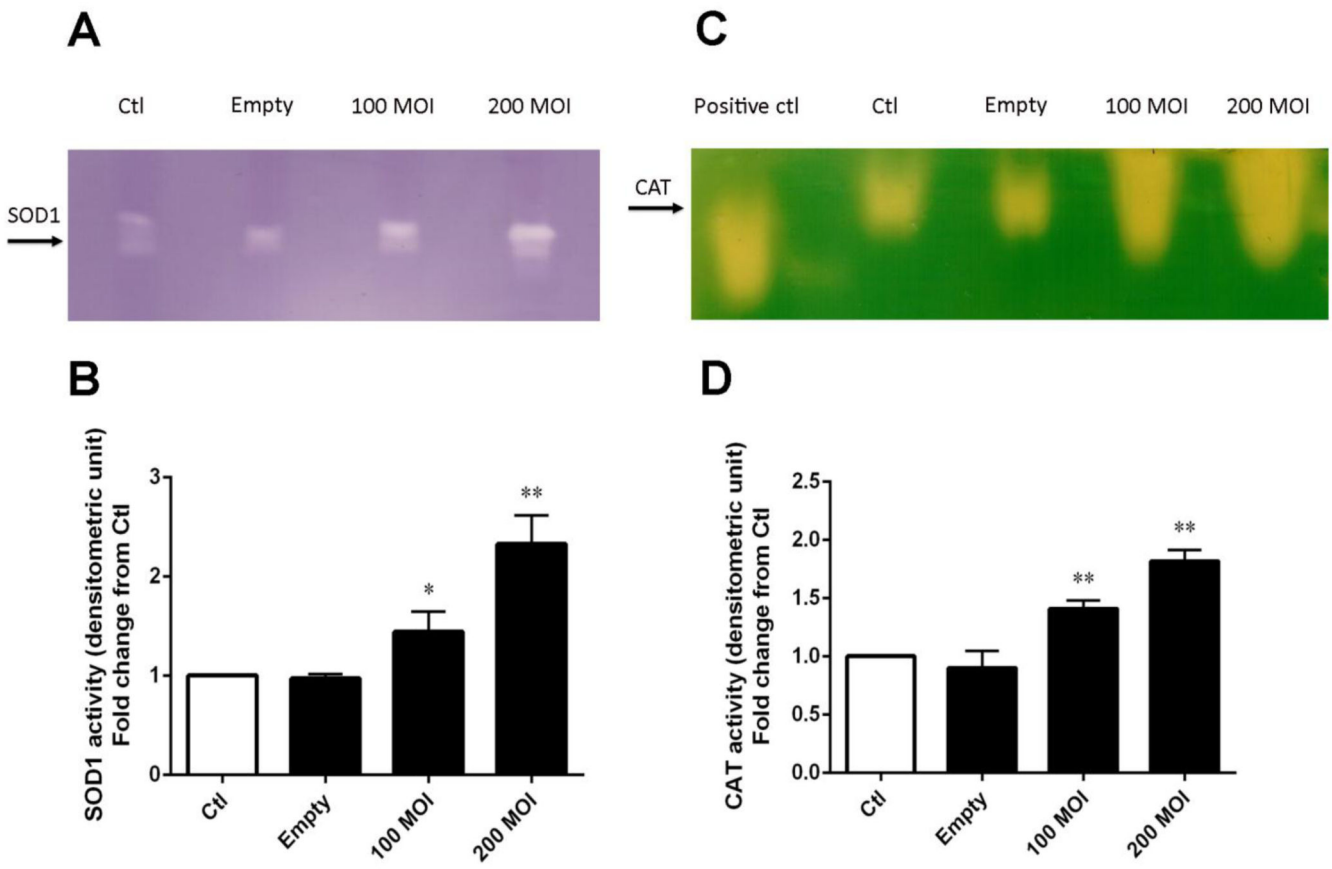

Figure 2. Recombinant adenovirus produces active SOD1 or catalase proteins

(**A**) Representative SOD1 activity gel. (**B**) Densitometric analysis of SOD1 activities with different MOIs. The mean OD of the reactive bands in the control group was normalized to 1.0. (**C**) Representative catalase activity gel. (**D**) Densitometric analysis of catalase activity obtained with different MOIs. Catalase (1000 ng) from bovine liver used as a positive control. The mean OD of the reactive bands in the control group was normalized to 1.0. Data represent mean ± SD from 3 independent experiments. * $p < 0.05$, ** $p < 0.01$ compared to control group, as analyzed with ANOVA followed by two-tailed Student's *t*-test.

Author Manuscript Author Manuscript Author Manuscript Author Manuscript

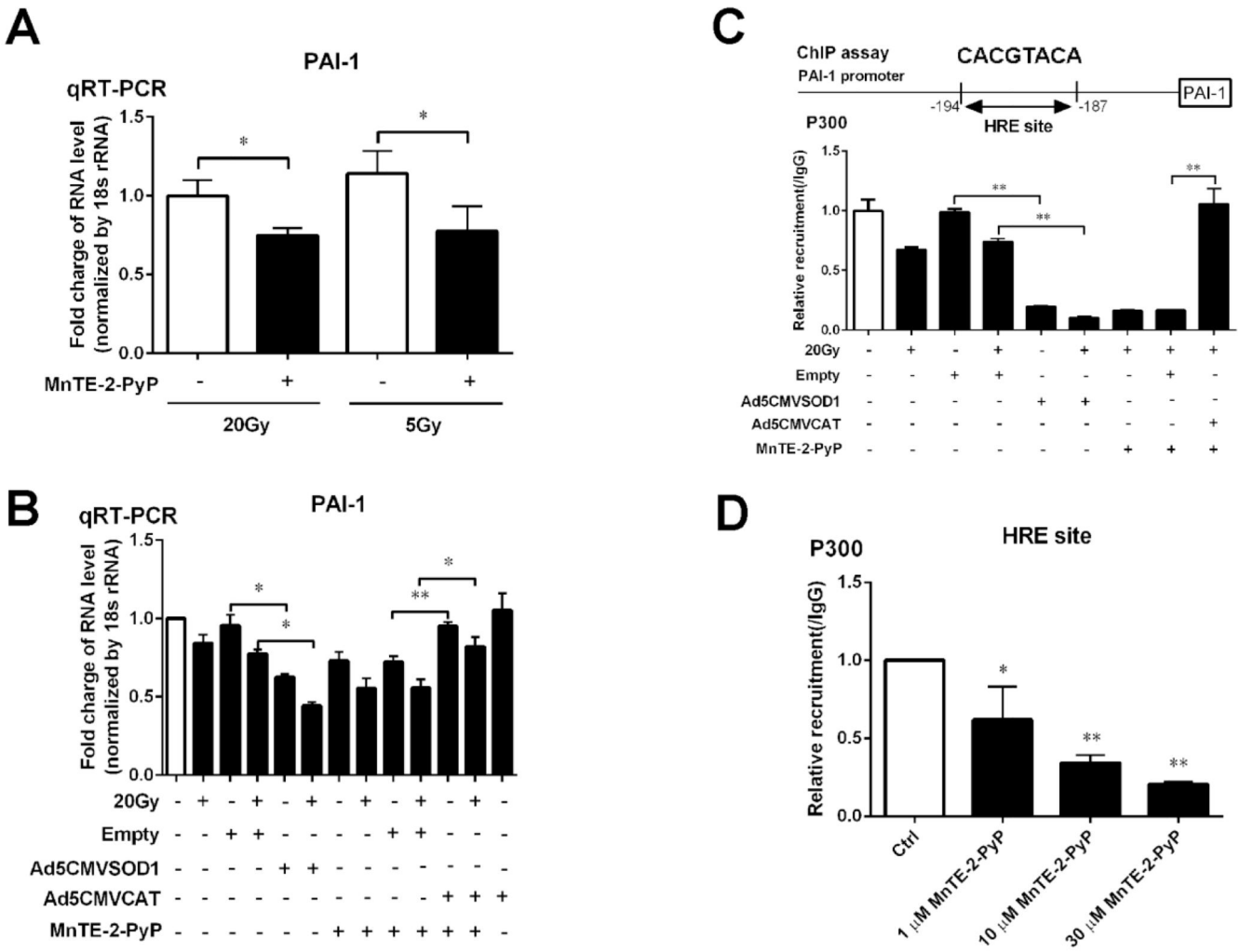

Figure 3. Effects of antioxidant proteins SOD1 and catalase on the expression of PAI-1 gene and the affinity of p300 association to DNA

(A) MnTE-2-PyP reduces PAI-1 gene expression with 20 Gy and 5 Gy of radiation. The gene expression levels of PAI-1 was measured by real-time PCR using the ΔΔCT method. 18S was used as the housekeeping gene. **(B)** PAI-1 mRNA expression in PC3 cells overexpressing SOD1 or catalase. Cells were exposed to 20 Gy of radiation. 24 hours later, RNA was isolated from PC3 cells and relative levels of human PAI-1 mRNA were analyzed by quantitative RT-PCR using the ΔΔCT method. 18S was used as the housekeeping gene. **(C)** Affinity for p300 to the HRE binding site on PAI-1 gene promoter region changes after SOD1 and catalase transfection. **(D)** MnTE-2-PyP inhibits p300 binding to the PAI-1 promoter in a dose dependent manner. Data represent mean ± SD from 3 independent experiments. * $p < 0.05$, ** $p < 0.01$ compared to control groups, as analyzed with ANOVA followed by two-tailed Student's *t*-test.

Author Manuscript Author Manuscript Author Manuscript Author Manuscript

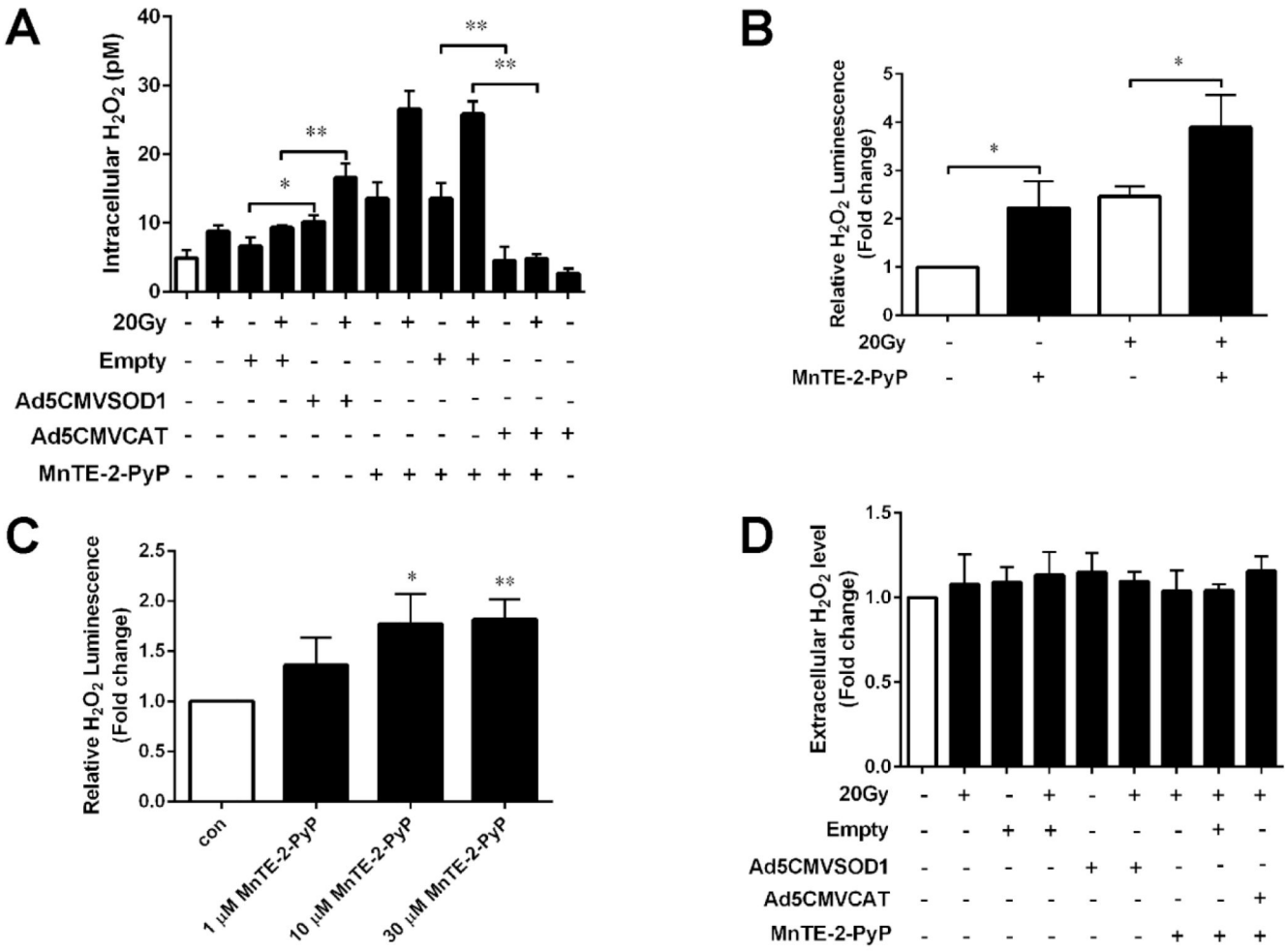

Figure 4. Various measurements of hydrogen peroxide levels following transfection with SOD1 or catalase adenovirus or treatment with MnTE-2-PyP with or without irradiation

(A) Detection of intracellular H_2O_2 in PC3 cells after transfection with SOD1, catalase adenovirus or treatment with MnTE-2-PyP. A 3-aminotriazole inhibition of catalase assay was performed to detect intracellular steady state levels of H_2O_2. **(B)** Intra and extracellular H_2O_2 levels measured by the ROS-GLO assay following MnTE-2-PyP treatment with or without 20 Gy radiation. **(C)** H_2O_2 levels measured by the ROS-GLO assay in PC3 cells treated with different doses of MnTE-2-PyP (1 μM, 10 μM and 30 μM). **(D)** Extracellular H_2O_2 concentration was measured by Amplex Red Hydrogen Peroxide Assay after transfection with SOD1, catalase adenovirus or treatment with MnTE-2-PyP. The mean H_2O_2 level in the blank control group was normalized to 1.0. Data represent mean ± SD from 3 independent experiments. * $p < 0.05$, ** $p < 0.01$ compared to control groups, as analyzed with ANOVA followed by two-tailed Student's *t*-test.

Author Manuscript Author Manuscript Author Manuscript Author Manuscript

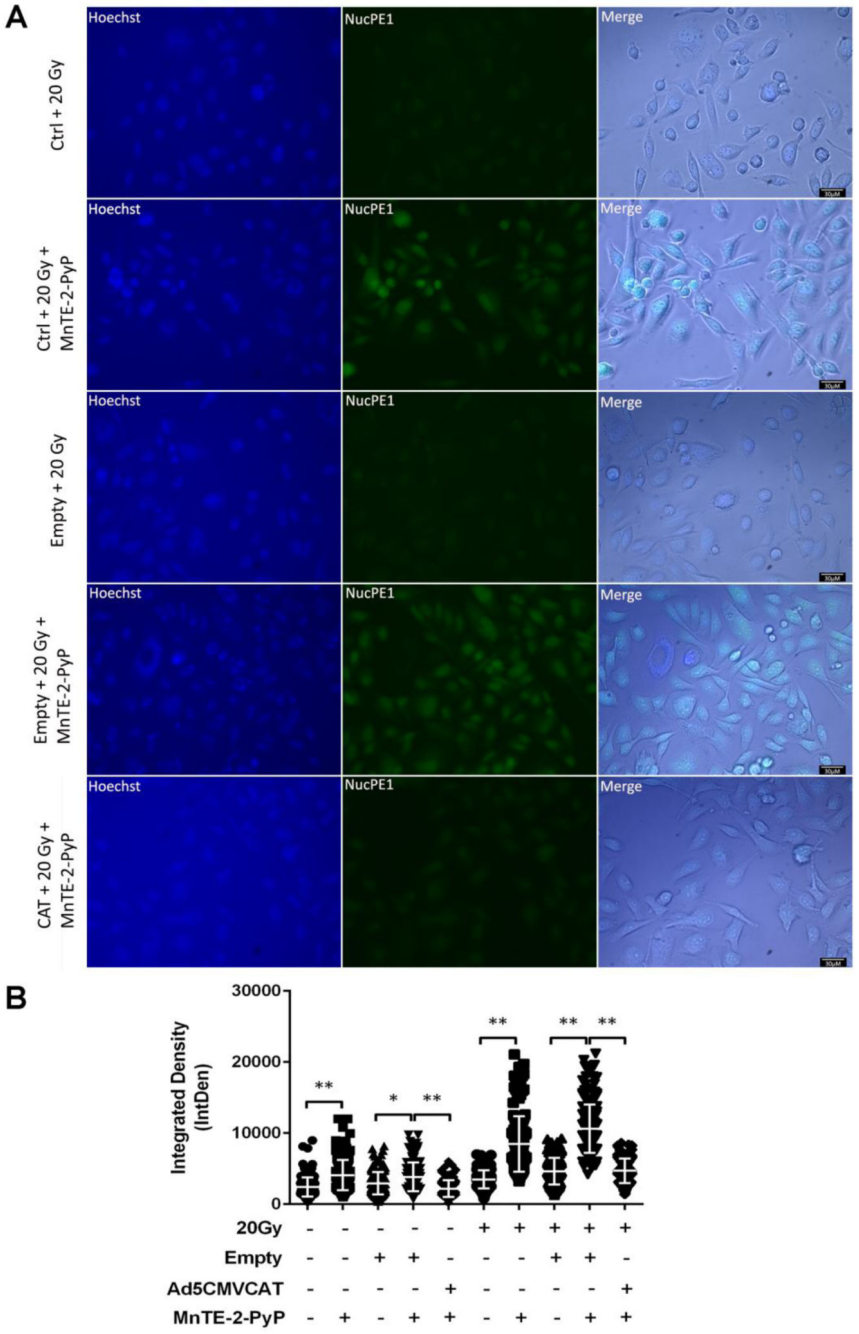

Figure 5. Nuclear localization and concentration of hydrogen peroxide levels

(A) Representative images of induced H_2O_2 in PC3 cells following MnTE-2-PyP treatment with or without catalase overexpression in the presence of radiation. Cells were imaged one hour post-radiation. Scale bar is 30 μm. **(B)** Integrated density analysis of H_2O_2 levels inside the nucleus with or without irradiation. The combined data is presented here as mean and std dev. ** $p < 0.01$, significance was determined with ANOVA followed by two-tailed Student's *t*-test.

Author Manuscript Author Manuscript Author Manuscript Author Manuscript

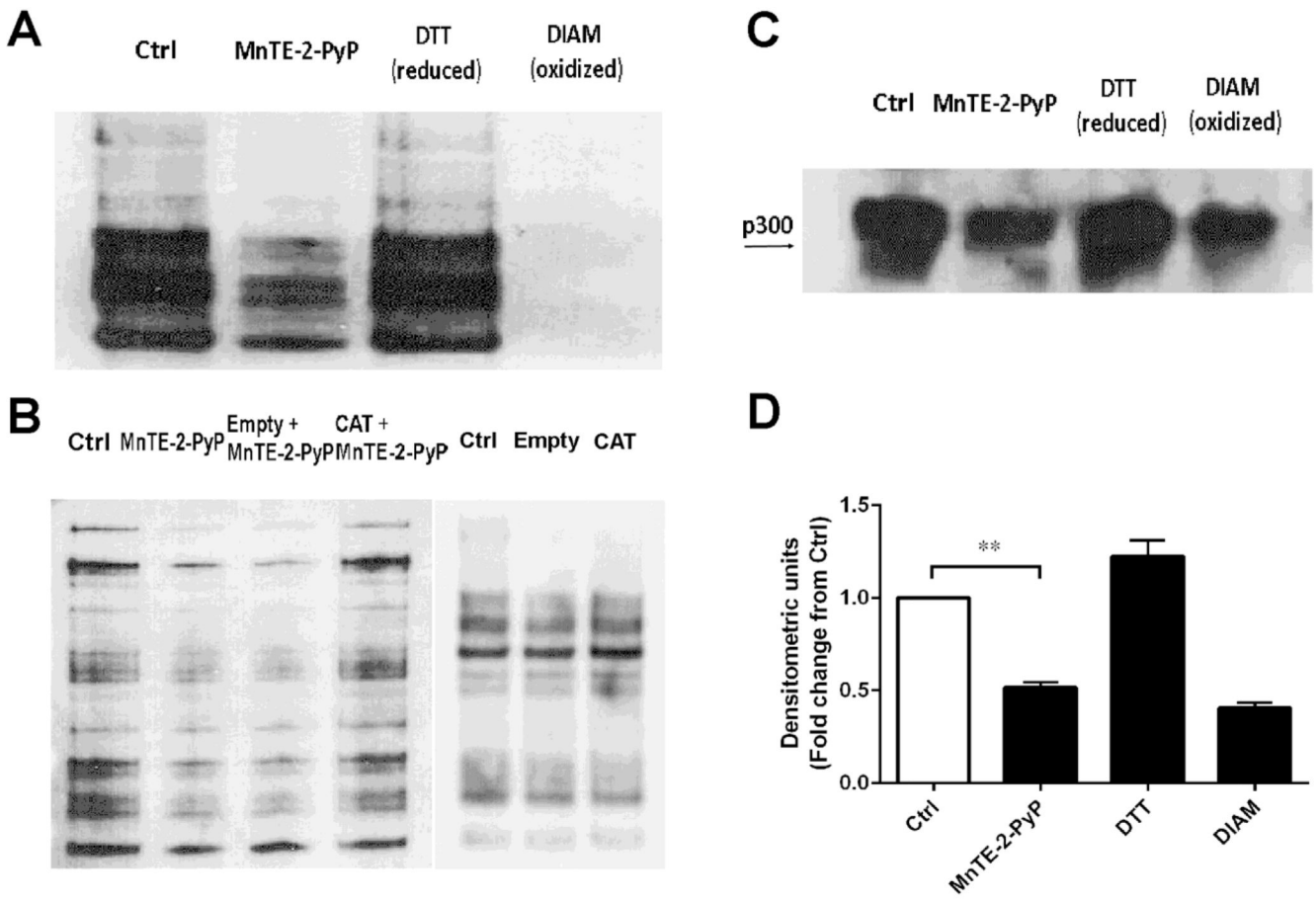

Figure 6. MnTE-2-PyP increased the oxidation of many proteins, including p300

(**A**) Total reduced thiols from whole cell lysates treated with or without MnTE-2-PyP. As a control, the lysates were treated with the reducing agent DTT and or oxidizing agent diamide (DIAM). (**B**) Thiol oxidation changes of whole proteins following catalase transfection in PC3 cells with or without MnTE-2-PyP treatment. (**C**) Measurement of reduced thiols present on p300 with or without MnTE-2-PyP. Biotinylated proteins were immunoprecipitated with streptavidin-agarose following by a p300 western blot. (**D**) Densitometric analysis of p300 western blots treated with or without MnTE-2-PyP. The mean OD of the reactive bands in the control group was normalized to 1.0. Data represent mean ± SD from 3 independent experiments. ** $p < 0.01$ compared to control group, as analyzed with ANOVA followed by two-tailed Student's *t*-test.